Supplementary for High capture capacity of CO_2 in nickel intercalated $Ti_3C_2T_x$ MXene-Fluorohectorite clay heterostructure

Barbara Pacakova,[*a] Anupma Thakur [b], Nithin Chandran B.S.[b], Nicolas Heymans[c], Irena Matulková[e], Hanna Demchenko[a], Alexander Harold Saxton[a], Kristoffer Hunvik[a], Guy De Weireld[c], Babak Anasori[b,d], Steinar Raaen[a] and Jon Otto Fossum [a]

[a]*Dept. of Physics, Norwegian University of Science and Technology, Hogskoleringen 5, 7034 Trondheim, Norway.*
[b]*School of Materials Engineering, Purdue University, West Lafayette, IN 47907, United States.*
[c]*Thermodynamics and Mathematical Physics Unit, University of Mons (UMONS), Place du parc 20, 7000 Mons, Belgium*
[d]*School of Mechanical Engineering, Purdue University, West Lafayette, IN 47907, United States*
[e]*Charles University, Faculty of Science, Department of Inorganic Chemistry, Hlavova 8, 128 40 Prague 2, Czech Republic*

1. Details of experimental methods

1.1 AFM

For the AFM measurements, 0.1 wt% water solution of delaminated clay nanosheets was drop-casted on plasma functionalized Si@SiO_2(100 nm) substrate. The sample was scanned using MultiMode AFM operating with the Nanoscope III controler. Images were captured in tapping mode, using TAP190Al-G AFM probes purchased from Budget Sensors. Images were processed using Gwyddion software[1] by aligning rows, flattening and scar corrections.

1.2 Gravimetry

Before measurement, the sample was outgassed at 120 °C for 3 hours under secondary vacuum. The pressure is measured with Tecsis-Series P3382. The temperature was recorded with Pt-100 sensor placed close to the sample crucible. The complete system is placed into a heating chamber to maintain constant temperature within 23 ± 0.5 °C. The suspension balance has a resolution of 10 μG. The sample mass variation m_{meas} (g) is measured as well as pressure and temperature when equilibrium is reached (with our criterion, when four of the five last mass measurements (noticed each 5 min) are included in an interval of 50 μg). The measured quantity is the excess adsorbed amount, which is obtained by correcting for the buoyancy of the skeletal volume of the sample material and the suspended metal parts. This volume is evaluated by a direct helium buoyancy effect measurement, according to helium not adsorbed at high pressure (10 bar up to 100 bar). The gas phase densities were determined using the equation of state for CO_2 [2] and Helium [3].

2. Additional data

2.1 Atomic force microscopy

Synthetic fluorohectorite clay

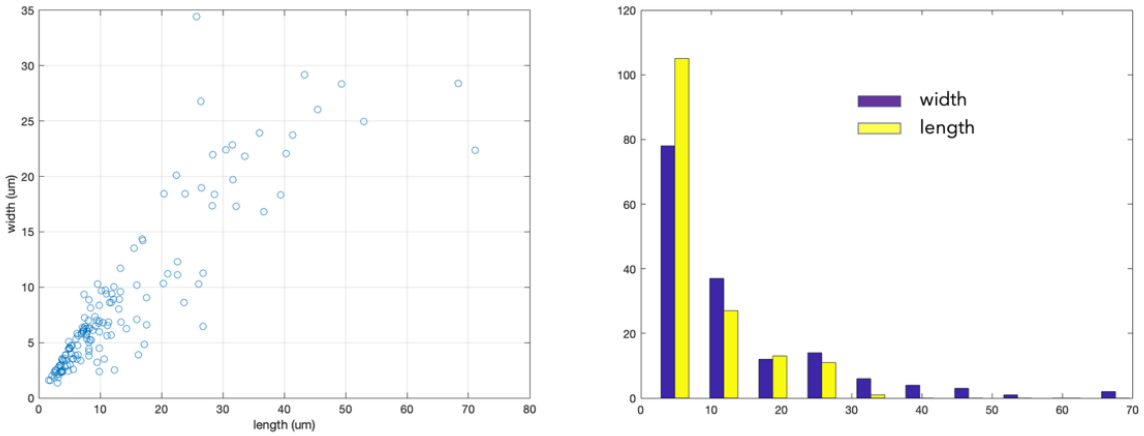

Figure S1. Left: width and length of the individual single Fht nanosheets. Right: histogram of the widths and lengths of all flakes.

$Ti_3C_2T_x$ MXene

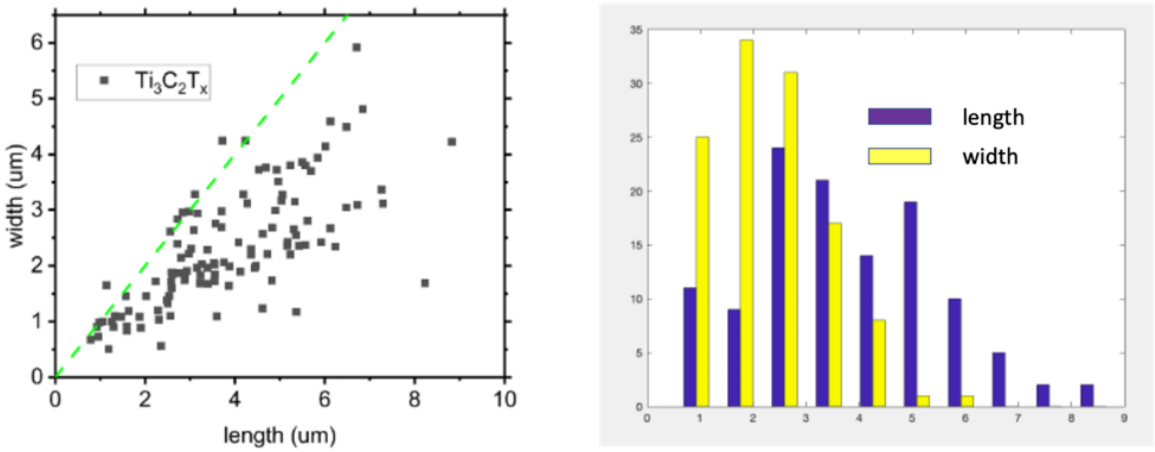

Figure S2. Left: width and length of the individual single MXene flakes. Right: histogram of the widths and lengths of all flakes.

2.2 CO_2 capture in Ni-$Ti_3C_2T_x$ reference sample

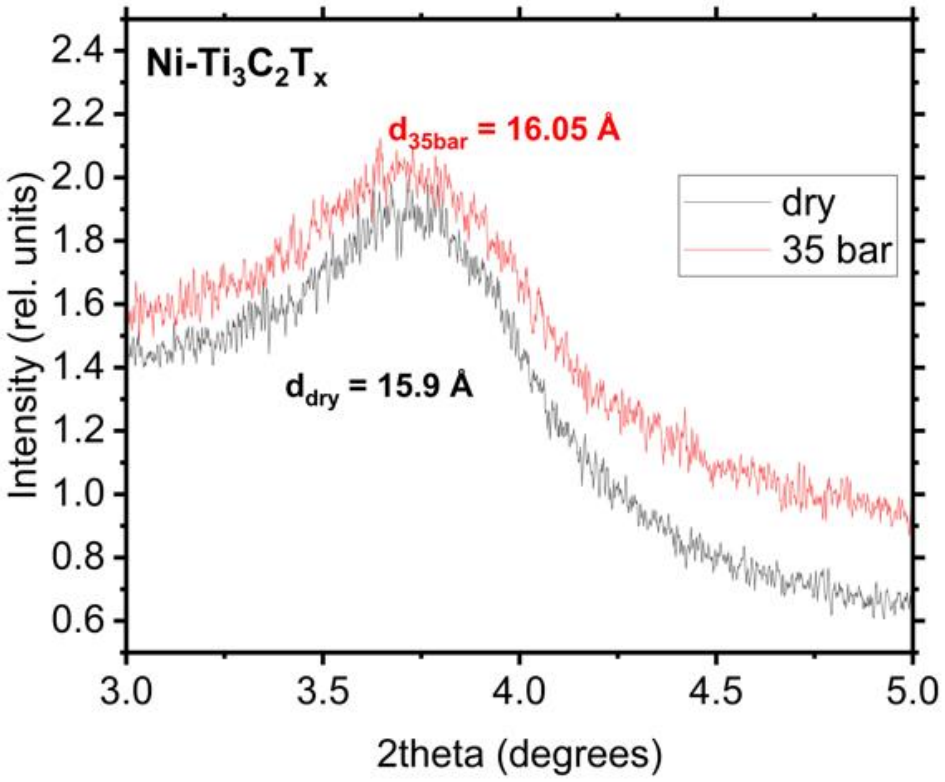

Figure S3. Synchrotron X-ray diffraction pattern of Ni-$Ti_3C_2T_x$ MXene sample in dry state and exposed to 35 bars.

2.3 Infrared spectroscopy

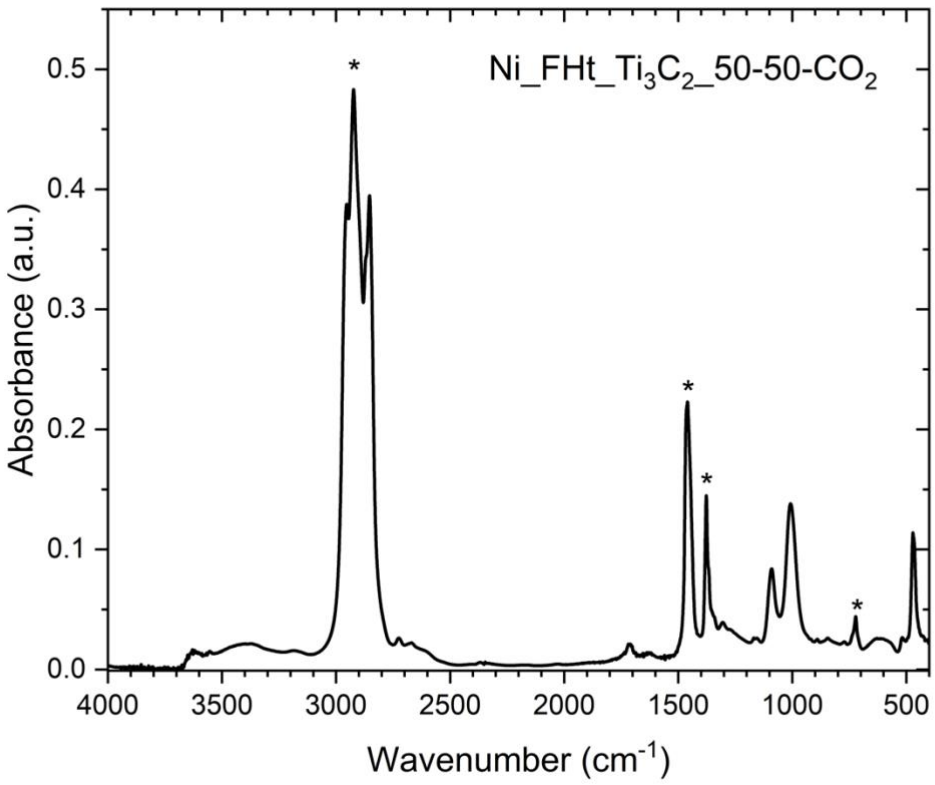

Figure S4. FTIR spectra of the Ni-MXene-clay heterostructure.

The best FTIR spectra were measured by the transmission technique. The bands marked by an asterisk are assigned to the vibrational bands of nujol (paraffinum liquidum). The bands at 1090, 1008, and 471 cm^{-1} in the **Ni-FHt-Ti_3C_2-50/50 CO_2** FTIR spectrum are associated with the vibrational behaviour of layered silicate. The broad bands in the region 3700-3200 cm^{-1} can be assigned to the stretching vibration of O-H bonds of α-$Ni(OH)_2$ involved in hydrogen interactions in the FTIR spectrum.
Unfortunately, the presence of CO_2 in the **Ni-FHt-Ti_3C_2-50/50 CO_2** sample cannot be verified by the method FTIR.

3. Summary of CO_2 adsorption capacity for different materials

Adsorbent	CO_2 adsorption capacity (mmol g^{-1})	Temperature (°C)	Pressure (bar)	References
Zeolites				[4]
Sodium type X zeolite (NaX)	*5.39*	25	1	[5]
Zeolite 13X (13x-c)	*6.2*	298 K	1	[6,7]
Zeolite 13X (13X-B)	*4.8*		1	[7]
Zeolite 4A	*6.217*	298 K	1	[8]
Zeolite 5A	*3.68*	298 K	1	[9]
Zeolite molecular sieve type 5A (5A)	3.88	30	10	[10]
	5.02	32	5	[11]
Lithium type X zeolite (LiX)	*5.51*	20	9	[12]
Zeolite molecular sieve type 13X (13X)	4.51	25	29	[13]
	5.87	32	2	[14]
	7.21	25	20	[15]
	0.0052	25	15	[16]
Zeolite Socony Mobil-5 (ZSM-5)	*2.50*	30	5.7	[17]
	0.90	40	1	[18]
Mobil Composition of Matter No. 41 (MCM-41)	0.53	30	1	[19]
	0.63	25	1	[20]
Mobil Composition of Matter No. 48 (MCM-48)	0.32	25	-	[21]
Santa Barbara Amorphous No. 15 (SBA-15)	0.40	25	1	[22]
Korea Advanced Institute of Science and Technology no.6 (KIT-6)	0.48	30	1	[23]
MOFs				[24–26]
Hong Kong University of Science and Technology-1 (HKUST-1)	7.19	30	10	[27]
	15.50	22	30	[28]
	3.60	25	1	[29]
Materials of Institute Lavoisier-101 (MIL-101)	0.85	25	10	[30]
	2.90	30	1.13	[31]
	1.17	30	2.41	[27]
	8.07	30	10	[27]
	21.28	22	36	[28]
	34	30	50	[28,32]
	40	30	50	
Metal organic framework-5 (MOF-5)	2.10	23	1	[33]
	15.22	24	14	[34]
MOF-210	54.5	298 K	50	[35]
	43.1		1	
MOF-177	33.5	298 K	35	[36]
	0.8		1	[36]
MOF-2	3.2		35	[36]
	0.7		1	
MOF-505	10.2		35	[36]
	3.3		1	
MOF-74	10.4		35	[36]
	4.9		1	
Ni-Datz-MOF-74	7.76		1	[37]
Cu3(BTC)2	10.7		35	[36]
	4.1		1	
IRMOF-11	14.7		35	[36]
	1.8		1	
IRMOF-3	18.7		35	[36]
	1.2		1	

IRMOF-6	19.5		35	[36]
	1.1		1	
IRMOF-1	21.7		35	[36]
	1.1		1	
Targeted modification of the metal sites				[26]
Mg_2(dobdc)	8-9	25	1	[6,38–42]
Mg_2(dobpdc)	6.42	25	1	[43]
Ni_2(dobdc)	7	25	1	[40,44]
Fe_2(dobdc)	7.1	25	1	[40,45]
Co_2(dobdc)	6.9	25	1	[39,40,44]
Zn_2(dobdc)	~5.61	25	1	[39,40,44]
Mn_2(dobdc)	~5.9	25	1	[40]
Cu_2(dobdc)	~2.90	25	1	
Mg_2(dondc)	6.42	25	1	[46]
Mg_2(dotpdc)	~5.30	25	1	[47]
Mg_2(pc-dobpdc)	~6.50	25	1	[47]
Mn_2(dobpdc)		25	1	[48]
Co_2(dobpdc)		25	1	[48]
Ni_2(dobpdc)		25	1	[48]
Zn_2(dobpdc)		25	1	[48]
Mg/Zn(dobdc)	5.10	25	1	[49]
Ni/Zn(dobdc)	4.80	25	1	[49]
Mg/Zn(dobpdc)	~5.90	25	1	[50]
SIFSIX-3-Cu	2.58	25	1	[38,51]
SIFSIX-3-Zn	2.51	25	1	[38,52]
SIFSIX-3-Ni	2.5	25	1	[6]
SIFSIX-18-Ni-β		25	1	[53]
SIFSIX-2-Cu-i	5.41	25	1	[38,51,52]
HKUST-1	2.5\4.1	25	1	[6,36]
UTSA-16	4.3	25	1	[54]
MIL-101(Cr)	1.22	25	1	[55]
ZU-16-Co	2.87	25	1	[56]
TIFSIX-3-Ni	2.32	25	1	[53,56,57]
NbOFFIVE-1-Ni	2.2	25	1	[53,58]
SIFSIX-14-Cu-i	4.70	25	1	[59]
dptz-CuTiF6	~4.51	25	1	[60]
MIL-53(Al)	2.58	25	1	[38,51]
Amorphous/activated carbon				[25,61]
Walnut shell	1.86	25	1	[62]
Cotton wood	1.61	25	1	[63]
Rambutan peel	1.72	25	1	[64]
Chicken manure	10.15	20	1	[65]
Rice husk char	3.1	25	1	[66]
Date seeds	2.94	25	1	[67]
Olive stones	3.1	25	1	[68]
Coconut shell	3.9	25	1	[69]
nutshell	3.48	25	1	[70]
Palm date seeds	4.38	25	1	[71]
Urea and tobacco stem	29.5	25	30	[72]
Carrot peels	4.18	25	1	[73]
Camellia japonica	5	25	1	[74]
Pristine gelatine and starch	3.84	25	1	[75]
Paulownia sawdust	5.8	25	1	[76]
Argan hard shells	5.63	25	1	[77]
Coffee grounds	6.89	25	1	[78]
Wooden chopstics	2.63	25	1	[79]
Polypodium vulgare	5.67	25	1	[80]
Lignin waste	2.4	25	1	[81]
Starch, cellulose and sawdust	4.8	25	1	[82]
Coconut shell-derived AC	0.18	20	1	[83]
	2.50	25	1	
	3.60	25	1	
	3.90	25	1	[69]

Oil palm biomass-derived AC	4.40	25	1	[84]
	3.71	25	1	[85]
Olive stone-derived AC	2.02	25	1	[86]
	3.10	25	1	[68]
Almond shell-derived AC	2.09	25	1	[86]
	2.70	25	1	[68]
Peanut shell-derived AC	4.41	25	1	[87]
Sawdust-derived AC	4.80	25	1	[76]
Bamboo-derived AC	4.50	25	1	[88]
Rice husk-derived AC	3.87	25	1	[89]
Coffee ground wastes-derived AC	2.67	35	1	[90]
	2.95	25	1.20	[91]
	2.90	25	1	[92]
Corn cob-derived AC	3.56	28	1	[93]
Wood-derived AC	4.10	30	1	[94]

COF

Covalent triazine framework-1 (CTF-1)	2.25	25	1	[95]
Perfluorinated triazine-based COF (FCFT-1)	3.41	25	1	[95]
Dual functional (3-aminopropyl) triethoxysilane-based COF (APTES-COF-1)	3.99	30	37	[96]
				[25]
TMFPT-COF	0.86	25	1	[97]
TPE-COF-II	5.27	0	1	[98]
cCTF-500	1.82	25	1	[99]
cCTF-400	1.89	25	1	[99]
[HO]25%-H2P-COF	31	25	1	[100]
[HO2C]100%-H2PeCOF	76	25	1	[100]

Silicates

[25]

SiO2-NS (Polyethyleneimine)	4.01	75	1	[101]
SBA-15 (Polyethyleneimine)	0.83	25	1	[102]
Silica monoliths (Tetraethylenepentamine)	2.23	25	1	[103]
Silica powder (Tetraethylenepentamine)	2.56	25	1	[103]
KIL-2 (Polyethyleneimine)	2.19	25	1	[104]
MSU-J (Tetraethylenepentamine)	3.73	25	1	[105]
Granular silica (Polyethyleneimine)	2.39	25	1	[106]
Microspherical silica (Polyethyleneimine)	2.27	25	1	[106]
Silica powder (3-aminopropyltrimethoxysilane	1.14	25	1	[103]
SBA-15 N1-(3-trimethoxysilylpropyl) diethylenetriamine	1.88	25	1	[107]

Carbon nanostructures

Mesoporous carbon nitride (CN) spheres	2.90	25	-	[108]
N-doped ordered mesoporous carbons (NMCs)	3.20	25	1	[109]
Resorcinol-formaldehyde (RF)-based carbon	3.13	25	1	[110]
Polyamide (PAN)-based ACF	1.92	25	1	[111]
Pitch-based ACFs	3.50	25	1	[112]
Graphene-based monolith	2.10	25	1	[113]
Mesophase pitches-based CMS	4.70	25	1	[114]
Cylindrical pelletized CMS	2.01	25	0.97	[115]
	3.43	25	9.99	
Polymeric based CMS	3.29	25	1	[116]
				[25]

PEI-graphite oxide APTS-graphite (Polyethyleneimine)	0.75	25	1	[117]
Graphite nanoplatelets (GNP)/Fe3O4	8.5	25	1	[118]
TEPA-graphite oxide	2.08	25	1	[119]
Graphite waste/Fe3O4	5.36	25	1	[118]
KOH activated graphite nanofibres	1.61, 1.35	25	1	[120,121]
MPD-graphene oxide	0.91	25	1	[122]
PEHA-graphene oxide	0.61	25	1	[122]
Monolithic reduced graphene oxide-based aerogels	6.31			[123]
TEPA-CNT	5.00	60	1	[124]
PEI-MWCNT	2.11	25	1	[125]
APS-CNT	2.19	25	1	[126]
MXenes				
Mo_2C-Li	***3.66***		4 Mpa	[127]
Mo_2C-Na	***3.47***			
Mo_2C-K	***3.31***			
Mo_2C-NH4	***3.34***			
Ti_3C_2	***1.33***		4 MPa	[128]
V_2C	***0.52***		4 MPa	[128]
DMSO-Ti_3C_2	***5.79***		4 MPa	[128]
DMSO-V_2C	***0.77***		4 MPa	[128]
Clays				
Cs-montmorillonite	1.4	-20	1	[129]
Cs-montmorillonite	0.9	20	1	[129]
Bentonite	0.23	10	10	[130]
Cs-Bentonite	1.25	10	10	
TMA-Bentonite	1.16	10	10	
MMA-Bentonite	0.92	10	10	
Mg, Cs and Ca -bentonite	0.6	20	1	[131]
Ni-fluorohectorite	***6.45***	20	55	[132]
Ni0.3-fluorohectorite	***2.14***	20	50	[133]

References

(1) Nečas, D.; Klapetek, P. Gwyddion: An Open-Source Software for SPM Data Analysis. *Central European Journal of Physics* 2012, *10* (1), 181–188. https://doi.org/10.2478/s11534-011-0096-2.

(2) Span, R.; Wagner, W. A New Equation of State for Carbon Dioxide Covering the Fluid Region from the Triple-Point Temperature to 1100 K at Pressures up to 800 MPa. *Journal of Physical and Chemical Reference Data*. 1996, pp 1509–1596. https://doi.org/10.1063/1.555991.

(3) Ortiz-Vega, D.; Hall, K.; Holste, J.; Arp, V.; Harvey, A.; Lemmon, E. Helmholtz Equation of State for Helium. *J Phys Chem Ref Data* 2020.

(4) Bahmanzadegan, F.; Ghaemi, A. Modification and Functionalization of Zeolites to Improve the Efficiency of CO2 Adsorption: A Review. *Case Studies in Chemical and Environmental Engineering* 2024, *9* (November 2023), 100564. https://doi.org/10.1016/j.cscee.2023.100564.

(5) Yan, B.; Yu, S.; Zeng, C.; Yu, L.; Wang, C.; Zhang, L. Binderless Zeolite NaX Microspheres with Enhanced CO2 Adsorption Selectivity. *Microporous and Mesoporous Materials* 2019, *278*, 267–274. https://doi.org/https://doi.org/10.1016/j.micromeso.2018.12.002.

(6) Kumar, A.; Madden, D. G.; Lusi, M.; Chen, K.-J.; Daniels, E. A.; Curtin, T.; Perry IV, J. J.; Zaworotko, M. J. Direct Air Capture of CO2 by Physisorbent Materials.

Angewandte Chemie International Edition 2015, *54* (48), 14372–14377. https://doi.org/https://doi.org/10.1002/anie.201506952.

(7) Hwang, K.-J.; Choi, W.-S.; Jung, S.-H.; Kwon, Y.-J.; Hong, S.; Choi, C.; Lee, J.-W.; Shim, W.-G. Synthesis of Zeolitic Material from Basalt Rock and Its Adsorption Properties for Carbon Dioxide. *RSC Adv* 2018, *8* (17), 9524–9529. https://doi.org/10.1039/C8RA00788H.

(8) Nguyen, T. H.; Kim, S.; Yoon, M.; Bae, T.-H. Hierarchical Zeolites with Amine-Functionalized Mesoporous Domains for Carbon Dioxide Capture. *ChemSusChem* 2016, *9* (5), 455–461. https://doi.org/10.1002/cssc.201600004.

(9) Chen, C.; Park, D.-W.; Ahn, W.-S. CO2 Capture Using Zeolite 13X Prepared from Bentonite. *Appl Surf Sci* 2014, *292*, 63–67. https://doi.org/10.1016/j.apsusc.2013.11.064.

(10) Mofarahi, M.; Gholipour, F. Gas Adsorption Separation of CO2/CH4 System Using Zeolite 5A. *Microporous and Mesoporous Materials* 2014, *200*, 1–10. https://doi.org/https://doi.org/10.1016/j.micromeso.2014.08.022.

(11) Mendes, P. A. P.; Ribeiro, A. M.; Gleichmann, K.; Ferreira, A. F. P.; Rodrigues, A. E. Separation of CO2/N2 on Binderless 5A Zeolite. *Journal of CO2 Utilization* 2017, *20*, 224–233. https://doi.org/https://doi.org/10.1016/j.jcou.2017.05.003.

(12) Park, Y.; Moon, D.-K.; Kim, Y.-H.; Ahn, H.; Lee, C.-H. Adsorption Isotherms of CO2, CO, N2, CH4, Ar and H2 on Activated Carbon and Zeolite LiX up to 1.0 MPa. *Adsorption* 2014, *20* (4), 631–647. https://doi.org/10.1007/s10450-014-9608-x.

(13) Zhang, Z.; Zhang, W.; Chen, X.; Xia, Q.; Li, Z. Adsorption of CO2 on Zeolite 13X and Activated Carbon with Higher Surface Area. *Sep Sci Technol* 2010, *45* (5), 710–719. https://doi.org/10.1080/01496390903571192.

(14) Kongnoo, A.; Tontisirin, S.; Worathanakul, P.; Phalakornkule, C. Surface Characteristics and CO2 Adsorption Capacities of Acid-Activated Zeolite 13X Prepared from Palm Oil Mill Fly Ash. *Fuel* 2017, *193*, 385–394. https://doi.org/https://doi.org/10.1016/j.fuel.2016.12.087.

(15) Garshasbi, V.; Jahangiri, M.; Anbia, M. Equilibrium CO2 Adsorption on Zeolite 13X Prepared from Natural Clays. *Appl Surf Sci* 2017, *393*, 225–233. https://doi.org/https://doi.org/10.1016/j.apsusc.2016.09.161.

(16) Chen, S. J.; Zhu, M.; Fu, Y.; Huang, Y. X.; Tao, Z. C.; Li, W. L. Using 13X, LiX, and LiPdAgX Zeolites for CO2 Capture from Post-Combustion Flue Gas. *Appl Energy* 2017, *191*, 87–98. https://doi.org/https://doi.org/10.1016/j.apenergy.2017.01.031.

(17) Frantz, T. S.; Ruiz, W. A.; da Rosa, C. A.; Mortola, V. B. Synthesis of ZSM-5 with High Sodium Content for CO2 Adsorption. *Microporous and Mesoporous Materials* 2016, *222*, 209–217. https://doi.org/https://doi.org/10.1016/j.micromeso.2015.10.022.

(18) Wang, Y.; Du, T.; Song, Y.; Che, S.; Fang, X.; Zhou, L. Amine-Functionalized Mesoporous ZSM-5 Zeolite Adsorbents for Carbon Dioxide Capture. *Solid State Sci* 2017, *73*, 27–35. https://doi.org/https://doi.org/10.1016/j.solidstatesciences.2017.09.004.

(19) Boonpoke, A.; Chiarakorn, S.; Laosiripojana, N.; Towprayoon, S.; Chidthaisong, A. Synthesis of Activated Carbon and MCM-41 from Bagasse and Rice Husk and Their Carbon Dioxide Adsorption Capacity. *Journal of Sustainable & Environment* 2013, *2*, 77–81.

(20) Ahmed, S.; Ramli, A.; Yusup, S. Development of Polyethylenimine-Functionalized Mesoporous Si-MCM-41 for CO2 Adsorption. *Fuel Processing Technology* 2017, *167*, 622–630. https://doi.org/https://doi.org/10.1016/j.fuproc.2017.07.036.

(21) Huang, H. Y.; Yang, R. T.; Chinn, D.; Munson, C. L. Amine-Grafted MCM-48 and Silica Xerogel as Superior Sorbents for Acidic Gas Removal from Natural Gas. *Ind Eng Chem Res* 2003, *42* (12), 2427–2433. https://doi.org/10.1021/ie020440u.
(22) WANG, L.; MA, L.; WANG, A.; LIU, Q.; ZHANG, T. CO2 Adsorption on SBA-15 Modified by Aminosilane. *Chinese Journal of Catalysis* 2007, *28* (9), 805–810. https://doi.org/https://doi.org/10.1016/S1872-2067(07)60066-7.
(23) Kishor, R.; Ghoshal, A. K. APTES Grafted Ordered Mesoporous Silica KIT-6 for CO2 Adsorption. *Chemical Engineering Journal* 2015, *262*, 882–890. https://doi.org/https://doi.org/10.1016/j.cej.2014.10.039.
(24) Das, A.; Peu, S. D.; Hossain, M. S.; Nahid, M. M. A.; Karim, F. R. Bin; Chowdhury, H.; Porag, M. H.; Argha, D. B. P.; Saha, S.; Islam, A. R. M. T.; Salah, M. M.; Shaker, A. Advancements in Adsorption Based Carbon Dioxide Capture Technologies- A Comprehensive Review. *Heliyon* 2023, *9* (12), e22341. https://doi.org/10.1016/j.heliyon.2023.e22341.
(25) Dziejarski, B.; Serafin, J.; Andersson, K.; Krzyżyńska, R. CO2 Capture Materials: A Review of Current Trends and Future Challenges. *Materials Today Sustainability* 2023, *24* (July). https://doi.org/10.1016/j.mtsust.2023.100483.
(26) Mahajan, S.; Lahtinen, M. Recent Progress in Metal-Organic Frameworks (MOFs) for CO2 Capture at Different Pressures. *J Environ Chem Eng* 2022, *10* (6), 108930. https://doi.org/10.1016/j.jece.2022.108930.
(27) Ye, S.; Jiang, X.; Ruan, L.-W.; Liu, B.; Wang, Y.-M.; Zhu, J.-F.; Qiu, L.-G. Post-Combustion CO2 Capture with the HKUST-1 and MIL-101(Cr) Metal–Organic Frameworks: Adsorption, Separation and Regeneration Investigations. *Microporous and Mesoporous Materials* 2013, *179*, 191–197. https://doi.org/https://doi.org/10.1016/j.micromeso.2013.06.007.
(28) Chowdhury, P.; Mekala, S.; Dreisbach, F.; Gumma, S. Adsorption of CO, CO2 and CH4 on Cu-BTC and MIL-101 Metal Organic Frameworks: Effect of Open Metal Sites and Adsorbate Polarity. *Microporous and Mesoporous Materials* 2012, *152*, 246–252. https://doi.org/https://doi.org/10.1016/j.micromeso.2011.11.022.
(29) Ba-Shammakh, M. S.; Sanna, A.; Maroto-Valer, M. M. Effect of Temperature, Dilute CO2 and MEA Impregnation on the CO2 Uptake of MIL-53 and HKUST-1 at Ambient Pressure. *Energy Procedia* 2017, *114*, 2405–2409. https://doi.org/https://doi.org/10.1016/j.egypro.2017.03.1387.
(30) Anbia, M.; Hoseini, V. Enhancement of CO2 Adsorption on Nanoporous Chromium Terephthalate (MIL-101) by Amine Modification. *Journal of Natural Gas Chemistry* 2012, *21* (3), 339–343. https://doi.org/https://doi.org/10.1016/S1003-9953(11)60374-5.
(31) Munusamy, K.; Sethia, G.; Patil, D. V; Somayajulu Rallapalli, P. B.; Somani, R. S.; Bajaj, H. C. Sorption of Carbon Dioxide, Methane, Nitrogen and Carbon Monoxide on MIL-101(Cr): Volumetric Measurements and Dynamic Adsorption Studies. *Chemical Engineering Journal* 2012, *195–196*, 359–368. https://doi.org/https://doi.org/10.1016/j.cej.2012.04.071.
(32) Llewellyn, P. L.; Bourrelly, S.; Serre, C.; Vimont, A.; Daturi, M.; Hamon, L.; De Weireld, G.; Chang, J.-S.; Hong, D.-Y.; Kyu Hwang, Y.; Hwa Jhung, S.; Férey, G. High Uptakes of CO2 and CH4 in Mesoporous Metal—Organic Frameworks MIL-100 and MIL-101. *Langmuir* 2008, *24* (14), 7245–7250. https://doi.org/10.1021/la800227x.
(33) Zhao, Z.; Li, Z.; Lin, Y. S. Adsorption and Diffusion of Carbon Dioxide on Metal−Organic Framework (MOF-5). *Ind Eng Chem Res* 2009, *48* (22), 10015–10020. https://doi.org/10.1021/ie900665f.
(34) Kloutse, F. A.; Hourri, A.; Natarajan, S.; Benard, P.; Chahine, R. Experimental Benchmark Data of CH4, CO2 and N2 Binary and Ternary Mixtures Adsorption on

MOF-5. *Sep Purif Technol* 2018, *197*, 228–236. https://doi.org/https://doi.org/10.1016/j.seppur.2018.01.013.
(35) Furukawa, H.; Ko, N.; Go, Y. B.; Aratani, N.; Choi, S. B.; Choi, E.; Yazaydin, A. Ö.; Snurr, R. Q.; O'Keeffe, M.; Kim, J.; Yaghi, O. M. Ultrahigh Porosity in Metal-Organic Frameworks. *Science (1979)* 2010, *329* (5990), 424–428. https://doi.org/10.1126/science.1192160.
(36) Millward, A. R.; Yaghi, O. M. Metal−Organic Frameworks with Exceptionally High Capacity for Storage of Carbon Dioxide at Room Temperature. *J Am Chem Soc* 2005, *127* (51), 17998–17999. https://doi.org/10.1021/ja0570032.
(37) Gao, S.; Feng, W.; Jin, J.; Mi, J.; Meng, H. Triazole-Functionalized Ni-MOF-74 for High-Performance CO2 Capture: Balancing Capacity, Selectivity, and Humidity Tolerance. *Chemical Engineering Journal* 2025, *515*, 163549. https://doi.org/https://doi.org/10.1016/j.cej.2025.163549.
(38) Shekhah, O.; Belmabkhout, Y.; Chen, Z.; Guillerm, V.; Cairns, A.; Adil, K.; Eddaoudi, M. Made-to-Order Metal-Organic Frameworks for Trace Carbon Dioxide Removal and Air Capture. *Nat Commun* 2014, *5* (1), 4228. https://doi.org/10.1038/ncomms5228.
(39) Caskey, S. R.; Wong-Foy, A. G.; Matzger, A. J. Dramatic Tuning of Carbon Dioxide Uptake via Metal Substitution in a Coordination Polymer with Cylindrical Pores. *J Am Chem Soc* 2008, *130* (33), 10870–10871. https://doi.org/10.1021/ja8036096.
(40) Queen, W. L.; Hudson, M. R.; Bloch, E. D.; Mason, J. A.; Gonzalez, M. I.; Lee, J. S.; Gygi, D.; Howe, J. D.; Lee, K.; Darwish, T. A.; James, M.; Peterson, V. K.; Teat, S. J.; Smit, B.; Neaton, J. B.; Long, J. R.; Brown, C. M. Comprehensive Study of Carbon Dioxide Adsorption in the Metal–Organic Frameworks M2(Dobdc) (M = Mg, Mn, Fe, Co, Ni, Cu, Zn). *Chem Sci* 2014, *5* (12), 4569–4581. https://doi.org/10.1039/C4SC02064B.
(41) Britt, D.; Furukawa, H.; Wang, B.; Glover, T. G.; Yaghi, O. M. Highly Efficient Separation of Carbon Dioxide by a Metal-Organic Framework Replete with Open Metal Sites. *Proceedings of the National Academy of Sciences* 2009, *106* (49), 20637–20640. https://doi.org/10.1073/pnas.0909718106.
(42) Bao, Z.; Yu, L.; Ren, Q.; Lu, X.; Deng, S. Adsorption of CO2 and CH4 on a Magnesium-Based Metal Organic Framework. *J Colloid Interface Sci* 2011, *353* (2), 549–556. https://doi.org/https://doi.org/10.1016/j.jcis.2010.09.065.
(43) McDonald, T. M.; Lee, W. R.; Mason, J. A.; Wiers, B. M.; Hong, C. S.; Long, J. R. Capture of Carbon Dioxide from Air and Flue Gas in the Alkylamine-Appended Metal–Organic Framework Mmen-Mg2(Dobpdc). *J Am Chem Soc* 2012, *134* (16), 7056–7065. https://doi.org/10.1021/ja300034j.
(44) Yazaydın, A. Ö.; Snurr, R. Q.; Park, T.-H.; Koh, K.; Liu, J.; LeVan, M. D.; Benin, A. I.; Jakubczak, P.; Lanuza, M.; Galloway, D. B.; Low, J. J.; Willis, R. R. Screening of Metal−Organic Frameworks for Carbon Dioxide Capture from Flue Gas Using a Combined Experimental and Modeling Approach. *J Am Chem Soc* 2009, *131* (51), 18198–18199. https://doi.org/10.1021/ja9057234.
(45) Märcz, M.; Johnsen, R. E.; Dietzel, P. D. C.; Fjellvåg, H. The Iron Member of the CPO-27 Coordination Polymer Series: Synthesis, Characterization, and Intriguing Redox Properties. *Microporous and Mesoporous Materials* 2012, *157*, 62–74. https://doi.org/https://doi.org/10.1016/j.micromeso.2011.12.035.
(46) Yeon, J. S.; Lee, W. R.; Kim, N. W.; Jo, H.; Lee, H.; Song, J. H.; Lim, K. S.; Kang, D. W.; Seo, J. G.; Moon, D.; Wiers, B.; Hong, C. S. Homodiamine-Functionalized Metal–Organic Frameworks with a MOF-74-Type Extended Structure for Superior Selectivity of CO2 over N2. *J Mater Chem A Mater* 2015, *3* (37), 19177–19185. https://doi.org/10.1039/C5TA02357B.

(47) Milner, P. J.; Martell, J. D.; Siegelman, R. L.; Gygi, D.; Weston, S. C.; Long, J. R. Overcoming Double-Step CO2 Adsorption and Minimizing Water Co-Adsorption in Bulky Diamine-Appended Variants of Mg2(Dobpdc). *Chem Sci* 2017, *9* (1), 160–174. https://doi.org/https://doi.org/10.1039/c7sc04266c.

(48) Yoo, G. Y.; Lee, W. R.; Jo, H.; Park, J.; Song, J. H.; Lim, K. S.; Moon, D.; Jung, H.; Lim, J.; Han, S. S.; Jung, Y.; Hong, C. S. Adsorption of Carbon Dioxide on Unsaturated Metal Sites in M2(Dobpdc) Frameworks with Exceptional Structural Stability and Relation between Lewis Acidity and Adsorption Enthalpy. *Chemistry - A European Journal* 2016, *22* (22), 7444–7451. https://doi.org/10.1002/chem.201600189.

(49) Kim, D.; Coskun, A. Template-Directed Approach Towards the Realization of Ordered Heterogeneity in Bimetallic Metal–Organic Frameworks. *Angewandte Chemie International Edition* 2017, *56* (18), 5071–5076. https://doi.org/https://doi.org/10.1002/anie.201702501.

(50) Kim, H.; Lee, H. Y.; Kang, D. W.; Kang, M.; Choe, J. H.; Lee, W. R.; Hong, C. S. Control of the Metal Composition in Bimetallic Mg/Zn(Dobpdc) Constructed from a One-Dimensional Zn-Based Template. *Inorg Chem* 2019, *58* (20), 14107–14111. https://doi.org/10.1021/acs.inorgchem.9b02126.

(51) Madden, D. G.; Scott, H. S.; Kumar, A.; Chen, K.-J.; Sanii, R.; Alankriti, B.; Lusi, M.; Curtin, T.; Perry, J. J.; Zaworotko, M. J. Flue-Gas and Direct-Air Capture of CO2 by Porous Metal–Organic Materials. *Phil. Trans. R. Soc. A.* 2017, 37520160025. https://doi.org/http://doi.org/10.1098/rsta.2016.0025.

(52) Nugent, P.; Belmabkhout, Y.; Burd, S. D.; Cairns, A. J.; Luebke, R.; Forrest, K.; Pham, T.; Ma, S.; Space, B.; Wojtas, L.; Eddaoudi, M.; Zaworotko, M. J. Porous Materials with Optimal Adsorption Thermodynamics and Kinetics for CO2 Separation. *Nature* 2013, *495* (7439), 80–84. https://doi.org/10.1038/nature11893.

(53) Mukherjee, S.; Sikdar, N.; O'Nolan, D.; Franz, D. M.; Gascón, V.; Kumar, A.; Kumar, N.; Scott, H. S.; Madden, D. G.; Kruger, P. E.; Space, B.; Zaworotko, M. J. Trace CO2 Capture by an Ultramicroporous Physisorbent with Low Water Affinity. *Sci Adv* 2025, *5* (11), eaax9171. https://doi.org/10.1126/sciadv.aax9171.

(54) Xiang, S.; He, Y.; Zhang, Z.; Wu, H.; Zhou, W.; Krishna, R.; Chen, B. Microporous Metal-Organic Framework with Potential for Carbon Dioxide Capture at Ambient Conditions. *Nat Commun* 2012, *3* (1), 954. https://doi.org/10.1038/ncomms1956.

(55) Chen, C.; Feng, N.; Guo, Q.; Li, Z.; Li, X.; Ding, J.; Wang, L.; Wan, H.; Guan, G. Surface Engineering of a Chromium Metal-Organic Framework with Bifunctional Ionic Liquids for Selective CO2 Adsorption: Synergistic Effect between Multiple Active Sites. *J Colloid Interface Sci* 2018, *521*, 91–101. https://doi.org/https://doi.org/10.1016/j.jcis.2018.03.029.

(56) Zhang, Z.; Ding, Q.; Cui, J.; Cui, X.; Xing, H. High and Selective Capture of Low-Concentration CO2 with an Anion-Functionalized Ultramicroporous Metal-Organic Framework. *Sci China Mater* 2021, *64* (3), 691–697. https://doi.org/10.1007/s40843-020-1471-0.

(57) Kumar, A.; Hua, C.; Madden, D. G.; O'Nolan, D.; Chen, K.-J.; Keane, L.-A. J.; Perry, J. J.; Zaworotko, M. J. Hybrid Ultramicroporous Materials (HUMs) with Enhanced Stability and Trace Carbon Capture Performance. *Chemical Communications* 2017, *53* (44), 5946–5949. https://doi.org/10.1039/C7CC02289A.

(58) Bhatt, P. M.; Belmabkhout, Y.; Cadiau, A.; Adil, K.; Shekhah, O.; Shkurenko, A.; Barbour, L. J.; Eddaoudi, M. A Fine-Tuned Fluorinated MOF Addresses the Needs for Trace CO2 Removal and Air Capture Using Physisorption. *J Am Chem Soc* 2016, *138* (29), 9301–9307. https://doi.org/10.1021/jacs.6b05345.

(59) Jiang, M.; Li, B.; Cui, X.; Yang, Q.; Bao, Z.; Yang, Y.; Wu, H.; Zhou, W.; Chen, B.; Xing, H. Controlling Pore Shape and Size of Interpenetrated Anion-Pillared Ultramicroporous Materials Enables Molecular Sieving of CO2 Combined with Ultrahigh Uptake Capacity. *ACS Appl Mater Interfaces* 2018, *10* (19), 16628–16635. https://doi.org/10.1021/acsami.8b03358.

(60) Liang, W.; Bhatt, P. M.; Shkurenko, A.; Adil, K.; Mouchaham, G.; Aggarwal, H.; Mallick, A.; Jamal, A.; Belmabkhout, Y.; Eddaoudi, M. A Tailor-Made Interpenetrated MOF with Exceptional Carbon-Capture Performance from Flue Gas. *Chem* 2019, *5* (4), 950–963. https://doi.org/https://doi.org/10.1016/j.chempr.2019.02.007.

(61) Gautam; Sahoo, S. Experimental Investigation on Different Activated Carbons as Adsorbents for CO2 Capture. *Thermal Science and Engineering Progress* 2022, *33*, 101339. https://doi.org/https://doi.org/10.1016/j.tsep.2022.101339.

(62) Lahijani, P.; Mohammadi, M.; Mohamed, A. R. Metal Incorporated Biochar as a Potential Adsorbent for High Capacity CO2 Capture at Ambient Condition. *Journal of CO2 Utilization* 2018, *26*, 281–293. https://doi.org/https://doi.org/10.1016/j.jcou.2018.05.018.

(63) Creamer, A. E.; Gao, B.; Wang, S. Carbon Dioxide Capture Using Various Metal Oxyhydroxide–Biochar Composites. *Chemical Engineering Journal* 2016, *283*, 826–832. https://doi.org/https://doi.org/10.1016/j.cej.2015.08.037.

(64) Zubbri, N. A.; Mohamed, A. R.; Kamiuchi, N.; Mohammadi, M. Enhancement of CO2 Adsorption on Biochar Sorbent Modified by Metal Incorporation. *Environmental Science and Pollution Research* 2020, *27* (11), 11809–11829. https://doi.org/10.1007/s11356-020-07734-3.

(65) Nguyen, M.-V.; Lee, B.-K. A Novel Removal of CO2 Using Nitrogen Doped Biochar Beads as a Green Adsorbent. *Process Safety and Environmental Protection* 2016, *104*, 490–498. https://doi.org/https://doi.org/10.1016/j.psep.2016.04.007.

(66) Li, M.; Xiao, R. Preparation of a Dual Pore Structure Activated Carbon from Rice Husk Char as an Adsorbent for CO2 Capture. *Fuel Processing Technology* 2019, *186*, 35–39. https://doi.org/https://doi.org/10.1016/j.fuproc.2018.12.015.

(67) Ogungbenro, A. E.; Quang, D. V; Al-Ali, K. A.; Vega, L. F.; Abu-Zahra, M. R. M. Physical Synthesis and Characterization of Activated Carbon from Date Seeds for CO2 Capture. *J Environ Chem Eng* 2018, *6* (4), 4245–4252. https://doi.org/https://doi.org/10.1016/j.jece.2018.06.030.

(68) González, A. S.; Plaza, M. G.; Rubiera, F.; Pevida, C. Sustainable Biomass-Based Carbon Adsorbents for Post-Combustion CO2 Capture. *Chemical Engineering Journal* 2013, *230*, 456–465. https://doi.org/https://doi.org/10.1016/j.cej.2013.06.118.

(69) Ello, A. S.; de Souza, L. K. C.; Trokourey, A.; Jaroniec, M. Coconut Shell-Based Microporous Carbons for CO2 Capture. *Microporous and Mesoporous Materials* 2013, *180*, 280–283. https://doi.org/https://doi.org/10.1016/j.micromeso.2013.07.008.

(70) Bae, J.-S.; Su, S. Macadamia Nut Shell-Derived Carbon Composites for Post Combustion CO2 Capture. *International Journal of Greenhouse Gas Control* 2013, *19*, 174–182. https://doi.org/https://doi.org/10.1016/j.ijggc.2013.08.013.

(71) Alazmi, A.; Nicolae, S. A.; Modugno, P.; Hasanov, B. E.; Titirici, M. M.; Costa, P. M. F. J. Activated Carbon from Palm Date Seeds for CO2 Capture. *International Journal of Environmental Research and Public Health*. 2021, p 12142. https://doi.org/10.3390/ijerph182212142.

(72) Ma, X.; Chen, R.; Zhou, K.; Wu, Q.; Li, H.; Zeng, Z.; Li, L. Activated Porous Carbon with an Ultrahigh Surface Area Derived from Waste Biomass for Acetone Adsorption, CO2 Capture, and Light Hydrocarbon Separation. *ACS Sustain Chem Eng* 2020, *8* (31), 11721–11728. https://doi.org/10.1021/acssuschemeng.0c03725.

(73) Serafin, J.; Narkiewicz, U.; Morawski, A. W.; Wróbel, R. J.; Michalkiewicz, B. Highly Microporous Activated Carbons from Biomass for CO2 Capture and Effective Micropores at Different Conditions. *Journal of CO2 Utilization* 2017, *18*, 73–79. https://doi.org/https://doi.org/10.1016/j.jcou.2017.01.006.
(74) Coromina, H. M.; Walsh, D. A.; Mokaya, R. Biomass-Derived Activated Carbon with Simultaneously Enhanced CO2 Uptake for Both Pre and Post Combustion Capture Applications. *J Mater Chem A Mater* 2016, *4* (1), 280–289. https://doi.org/10.1039/C5TA09202G.
(75) Alabadi, A.; Razzaque, S.; Yang, Y.; Chen, S.; Tan, B. Highly Porous Activated Carbon Materials from Carbonized Biomass with High CO2 Capturing Capacity. *Chemical Engineering Journal* 2015, *281*, 606–612. https://doi.org/https://doi.org/10.1016/j.cej.2015.06.032.
(76) Zhu, X.-L.; Wang, P.-Y.; Peng, C.; Yang, J.; Yan, X.-B. Activated Carbon Produced from Paulownia Sawdust for High-Performance CO2 Sorbents. *Chinese Chemical Letters* 2014, *25* (6), 929–932. https://doi.org/https://doi.org/10.1016/j.cclet.2014.03.039.
(77) Boujibar, O.; Souikny, A.; Ghamouss, F.; Achak, O.; Dahbi, M.; Chafik, T. CO2 Capture Using N-Containing Nanoporous Activated Carbon Obtained from Argan Fruit Shells. *J Environ Chem Eng* 2018, *6* (2), 1995–2002. https://doi.org/https://doi.org/10.1016/j.jece.2018.03.005.
(78) Travis, W.; Gadipelli, S.; Guo, Z. Superior CO2 Adsorption from Waste Coffee Ground Derived Carbons. *RSC Adv* 2015, *5* (37), 29558–29562. https://doi.org/10.1039/C4RA13026J.
(79) Phadungbut, P.; Koo-amornpattana, W.; Bumroongsri, P.; Ratchahat, S.; Kunthakudee, N.; Jonglertjunya, W.; Chalermsinsuwan, B.; Hunsom, M. Adsorptive Purification of CO2/H2 Gas Mixtures of Spent Disposable Wooden Chopstick-Derived Activated Carbon: Optimal Synthesis Condition. *Sep Purif Technol* 2022, *291*, 120948. https://doi.org/https://doi.org/10.1016/j.seppur.2022.120948.
(80) Serafin, J.; Kiełbasa, K.; Michalkiewicz, B. The New Tailored Nanoporous Carbons from the Common Polypody (Polypodium Vulgare): The Role of Textural Properties for Enhanced CO2 Adsorption. *Chemical Engineering Journal* 2022, *429*, 131751. https://doi.org/https://doi.org/10.1016/j.cej.2021.131751.
(81) Sangchoom, W.; Mokaya, R. Valorization of Lignin Waste: Carbons from Hydrothermal Carbonization of Renewable Lignin as Superior Sorbents for CO2 and Hydrogen Storage. *ACS Sustain Chem Eng* 2015, *3* (7), 1658–1667. https://doi.org/10.1021/acssuschemeng.5b00351.
(82) Sevilla, M.; Fuertes, A. B. Sustainable Porous Carbons with a Superior Performance for CO2 Capture. *Energy Environ Sci* 2011, *4* (5), 1765–1771. https://doi.org/10.1039/C0EE00784F.
(83) Hidayu, A. R.; Muda, N. Preparation and Characterization of Impregnated Activated Carbon from Palm Kernel Shell and Coconut Shell for CO2 Capture. *Procedia Eng* 2016, *148*, 106–113. https://doi.org/https://doi.org/10.1016/j.proeng.2016.06.463.
(84) Ello, A. S.; de Souza, L. K. C.; Trokourey, A.; Jaroniec, M. Development of Microporous Carbons for CO2 Capture by KOH Activation of African Palm Shells. *Journal of CO2 Utilization* 2013, *2*, 35–38. https://doi.org/https://doi.org/10.1016/j.jcou.2013.07.003.
(85) Parshetti, G. K.; Chowdhury, S.; Balasubramanian, R. Biomass Derived Low-Cost Microporous Adsorbents for Efficient CO2 Capture. *Fuel* 2015, *148*, 246–254. https://doi.org/https://doi.org/10.1016/j.fuel.2015.01.032.

(86) Plaza, M. G.; González, A. S.; Pis, J. J.; Rubiera, F.; Pevida, C. Production of Microporous Biochars by Single-Step Oxidation: Effect of Activation Conditions on CO2 Capture. *Appl Energy* 2014, *114*, 551–562. https://doi.org/https://doi.org/10.1016/j.apenergy.2013.09.058.
(87) Li, D.; Tian, Y.; Li, L.; Li, J.; Zhang, H. Production of Highly Microporous Carbons with Large CO2 Uptakes at Atmospheric Pressure by KOH Activation of Peanut Shell Char. *Journal of Porous Materials* 2015, *22* (6), 1581–1588. https://doi.org/10.1007/s10934-015-0041-7.
(88) Wei, H.; Deng, S.; Hu, B.; Chen, Z.; Wang, B.; Huang, J.; Yu, G. Granular Bamboo-Derived Activated Carbon for High CO2 Adsorption: The Dominant Role of Narrow Micropores. *ChemSusChem* 2012, *5* (12), 2354–2360. https://doi.org/https://doi.org/10.1002/cssc.201200570.
(89) Li, D.; Ma, T.; Zhang, R.; Tian, Y.; Qiao, Y. Preparation of Porous Carbons with High Low-Pressure CO2 Uptake by KOH Activation of Rice Husk Char. *Fuel* 2015, *139*, 68–70. https://doi.org/https://doi.org/10.1016/j.fuel.2014.08.027.
(90) Liu, S.-H.; Huang, Y.-Y. Valorization of Coffee Grounds to Biochar-Derived Adsorbents for CO2 Adsorption. *J Clean Prod* 2018, *175*, 354–360. https://doi.org/https://doi.org/10.1016/j.jclepro.2017.12.076.
(91) Plaza, M. G.; González, A. S.; Pevida, C.; Rubiera, F. Green Coffee Based CO2 Adsorbent with High Performance in Postcombustion Conditions. *Fuel* 2015, *140*, 633–648. https://doi.org/https://doi.org/10.1016/j.fuel.2014.10.014.
(92) Plaza, M. G.; González, A. S.; Pevida, C.; Pis, J. J.; Rubiera, F. Valorisation of Spent Coffee Grounds as CO2 Adsorbents for Postcombustion Capture Applications. *Appl Energy* 2012, *99*, 272–279. https://doi.org/https://doi.org/10.1016/j.apenergy.2012.05.028.
(93) Wang, Y. X.; Liu, B. S.; Zheng, C. Preparation and Adsorption Properties of Corncob-Derived Activated Carbon with High Surface Area. *J Chem Eng Data* 2010, *55* (11), 4669–4676. https://doi.org/10.1021/je1002913.
(94) Heidari, A.; Younesi, H.; Rashidi, A.; Ghoreyshi, A. Adsorptive Removal of CO2 on Highly Microporous Activated Carbons Prepared from Eucalyptus Camaldulensis Wood: Effect of Chemical Activation. *J Taiwan Inst Chem Eng* 2014, *45* (2), 579–588. https://doi.org/https://doi.org/10.1016/j.jtice.2013.06.007.
(95) Zhao, Y.; Yao, K. X.; Teng, B.; Zhang, T.; Han, Y. A Perfluorinated Covalent Triazine-Based Framework for Highly Selective and Water–Tolerant CO2 Capture. *Energy Environ Sci* 2013, *6* (12), 3684–3692. https://doi.org/10.1039/C3EE42548G.
(96) Du, Y.; Calabro, D.; Wooler, B.; Kortunov, P.; Li, Q.; Cundy, S.; Mao, K. One Step Facile Synthesis of Amine-Functionalized COF-1 with Enhanced Hydrostability. *Chemistry of Materials* 2015, *27* (5), 1445–1447. https://doi.org/10.1021/cm5032317.
(97) Li, X.; Su, Q.; Luo, K.; Li, H.; Li, G.; Wu, Q. Construction of a Highly Heteroatom-Functionalized Covalent Organic Framework and Its CO2 Capture Capacity and CO2/N2 Selectivity. *Mater Lett* 2021, *282*, 128704. https://doi.org/https://doi.org/10.1016/j.matlet.2020.128704.
(98) Gao, Q.; Li, X.; Ning, G.-H.; Xu, H.-S.; Liu, C.; Tian, B.; Tang, W.; Loh, K. P. Covalent Organic Framework with Frustrated Bonding Network for Enhanced Carbon Dioxide Storage. *Chemistry of Materials* 2018, *30* (5), 1762–1768. https://doi.org/10.1021/acs.chemmater.8b00117.
(99) Buyukcakir, O.; Je, S. H.; Talapaneni, S. N.; Kim, D.; Coskun, A. Charged Covalent Triazine Frameworks for CO2 Capture and Conversion. *ACS Appl Mater Interfaces* 2017, *9* (8), 7209–7216. https://doi.org/10.1021/acsami.6b16769.

(100) Huang, N.; Chen, X.; Krishna, R.; Jiang, D. Two-Dimensional Covalent Organic Frameworks for Carbon Dioxide Capture through Channel-Wall Functionalization. *Angewandte Chemie International Edition* 2015, *54* (10), 2986–2990. https://doi.org/https://doi.org/10.1002/anie.201411262.
(101) Shen, Z.; Cai, Q.; Yin, C.; Xia, Q.; Cheng, J.; Li, X.; Wang, Y. Facile Synthesis of Silica Nanosheets with Hierarchical Pore Structure and Their Amine-Functionalized Composite for Enhanced CO2 Capture. *Chem Eng Sci* 2020, *217*, 115528. https://doi.org/https://doi.org/10.1016/j.ces.2020.115528.
(102) Sanz, R.; Calleja, G.; Arencibia, A.; Sanz-Pérez, E. S. CO2 Adsorption on Branched Polyethyleneimine-Impregnated Mesoporous Silica SBA-15. *Appl Surf Sci* 2010, *256* (17), 5323–5328. https://doi.org/https://doi.org/10.1016/j.apsusc.2009.12.070.
(103) Thakkar, H.; Eastman, S.; Al-Mamoori, A.; Hajari, A.; Rownaghi, A. A.; Rezaei, F. Formulation of Aminosilica Adsorbents into 3D-Printed Monoliths and Evaluation of Their CO2 Capture Performance. *ACS Appl Mater Interfaces* 2017, *9* (8), 7489–7498. https://doi.org/10.1021/acsami.6b16732.
(104) Ojeda, M.; Mazaj, M.; Garcia, S.; Xuan, J.; Maroto-Valer, M. M.; Logar, N. Z. Novel Amine-Impregnated Mesostructured Silica Materials for CO2 Capture. *Energy Procedia* 2017, *114*, 2252–2258. https://doi.org/https://doi.org/10.1016/j.egypro.2017.03.1362.
(105) Jiao, J.; Cao, J.; Xia, Y.; Zhao, L. Improvement of Adsorbent Materials for CO2 Capture by Amine Functionalized Mesoporous Silica with Worm-Hole Framework Structure. *Chemical Engineering Journal* 2016, *306*, 9–16. https://doi.org/https://doi.org/10.1016/j.cej.2016.07.041.
(106) Zhang, H.; Goeppert, A.; Kar, S.; Prakash, G. K. S. Structural Parameters to Consider in Selecting Silica Supports for Polyethylenimine Based CO2 Solid Adsorbents. Importance of Pore Size. *Journal of CO2 Utilization* 2018, *26*, 246–253. https://doi.org/https://doi.org/10.1016/j.jcou.2018.05.004.
(107) Jahandar Lashaki, M.; Sayari, A. CO2 Capture Using Triamine-Grafted SBA-15: The Impact of the Support Pore Structure. *Chemical Engineering Journal* 2018, *334*, 1260–1269. https://doi.org/https://doi.org/10.1016/j.cej.2017.10.103.
(108) Li, Q.; Yang, J.; Feng, D.; Wu, Z.; Wu, Q.; Park, S. S.; Ha, C.-S.; Zhao, D. Facile Synthesis of Porous Carbon Nitride Spheres with Hierarchical Three-Dimensional Mesostructures for CO2 Capture. *Nano Res* 2010, *3* (9), 632–642. https://doi.org/10.1007/s12274-010-0023-7.
(109) Wei, J.; Zhou, D.; Sun, Z.; Deng, Y.; Xia, Y.; Zhao, D. A Controllable Synthesis of Rich Nitrogen-Doped Ordered Mesoporous Carbon for CO2 Capture and Supercapacitors. *Adv Funct Mater* 2013, *23* (18), 2322–2328. https://doi.org/https://doi.org/10.1002/adfm.201202764.
(110) Hao, G.-P.; Li, W.-C.; Qian, D.; Lu, A.-H. Rapid Synthesis of Nitrogen-Doped Porous Carbon Monolith for CO2 Capture. *Advanced Materials* 2010, *22* (7), 853–857. https://doi.org/https://doi.org/10.1002/adma.200903765.
(111) Chiang, Y.-C.; Hsu, W.-L.; Lin, S.-Y.; Juang, R.-S. Enhanced CO2 Adsorption on Activated Carbon Fibers Grafted with Nitrogen-Doped Carbon Nanotubes. *Materials*. 2017, p 511. https://doi.org/10.3390/ma10050511.
(112) Díez, N.; Álvarez, P.; Granda, M.; Blanco, C.; Santamaría, R.; Menéndez, R. CO2 Adsorption Capacity and Kinetics in Nitrogen-Enriched Activated Carbon Fibers Prepared by Different Methods. *Chemical Engineering Journal* 2015, *281*, 704–712. https://doi.org/https://doi.org/10.1016/j.cej.2015.06.126.

(113) Politakos, N.; Barbarin, I.; Cantador, L. S.; Cecilia, J. A.; Mehravar, E.; Tomovska, R. Graphene-Based Monolithic Nanostructures for CO2 Capture. *Ind Eng Chem Res* 2020, *59* (18), 8612–8621. https://doi.org/10.1021/acs.iecr.9b06998.
(114) Wahby, A.; Ramos-Fernández, J. M.; Martínez-Escandell, M.; Sepúlveda-Escribano, A.; Silvestre-Albero, J.; Rodríguez-Reinoso, F. High-Surface-Area Carbon Molecular Sieves for Selective CO2 Adsorption. *ChemSusChem* 2010, *3* (8), 974–981. https://doi.org/https://doi.org/10.1002/cssc.201000083.
(115) Park, Y.; Moon, D.-K.; Park, D.; Mofarahi, M.; Lee, C.-H. Adsorption Equilibria and Kinetics of CO2, CO, and N2 on Carbon Molecular Sieve. *Sep Purif Technol* 2019, *212*, 952–964. https://doi.org/https://doi.org/10.1016/j.seppur.2018.11.069.
(116) Wahby, A.; Silvestre-Albero, J.; Sepúlveda-Escribano, A.; Rodríguez-Reinoso, F. CO2 Adsorption on Carbon Molecular Sieves. *Microporous and Mesoporous Materials* 2012, *164*, 280–287. https://doi.org/https://doi.org/10.1016/j.micromeso.2012.06.034.
(117) Shin, G.-J.; Rhee, K.; Park, S.-J. Improvement of CO2 Capture by Graphite Oxide in Presence of Polyethylenimine. *Int J Hydrogen Energy* 2016, *41* (32), 14351–14359. https://doi.org/https://doi.org/10.1016/j.ijhydene.2016.05.162.
(118) Eny Kusrini Angga Kurniawan Sasongko,Nasruddin, anwar usman. Improvement of Carbon Dioxide Capture Using Graphite Waste/ Fe3O4 Composites. *International Journal of Technology* 2017, *8* (8), 291–319. https://doi.org/https://doi.org/10.14716/ijtech.v8i8.697.
(119) Zhang, Y.; Chi, Y.; Zhao, C.; Liu, Y.; Zhao, Y.; Jiang, L.; Song, Y. CO2 Adsorption Behavior of Graphite Oxide Modified with Tetraethylenepentamine. *J Chem Eng Data* 2018, *63* (1), 202–207. https://doi.org/10.1021/acs.jced.7b00824.
(120) Meng, L.-Y.; Park, S.-J. Effect of Heat Treatment on CO2 Adsorption of KOH-Activated Graphite Nanofibers. *J Colloid Interface Sci* 2010, *352* (2), 498–503. https://doi.org/https://doi.org/10.1016/j.jcis.2010.08.048.
(121) Yuan, H.; Meng, L.-Y.; Park, S.-J. KOH-Activated Graphite Nanofibers as CO2 Adsorbents. *Carbon Letters* 2016, *19* (1), 99–103. https://doi.org/10.5714/CL.2016.19.099.
(122) Hosseini, Y.; Najafi, M.; Khalili, S.; Jahanshahi, M.; Peyravi, M. Assembly of Amine-Functionalized Graphene Oxide for Efficient and Selective Adsorption of CO2. *Mater Chem Phys* 2021, *270*, 124788. https://doi.org/https://doi.org/10.1016/j.matchemphys.2021.124788.
(123) Yun, S.; Lee, H.; Lee, W.-E.; Park, H. S. Multiscale Textured, Ultralight Graphene Monoliths for Enhanced CO2 and SO2 Adsorption Capacity. *Fuel* 2016, *174*, 36–42. https://doi.org/https://doi.org/10.1016/j.fuel.2016.01.068.
(124) Irani, M.; Jacobson, A. T.; Gasem, K. A. M.; Fan, M. Modified Carbon Nanotubes/Tetraethylenepentamine for CO2 Capture. *Fuel* 2017, *206*, 10–18. https://doi.org/https://doi.org/10.1016/j.fuel.2017.05.087.
(125) Keller, L.; Ohs, B.; Lenhart, J.; Abduly, L.; Blanke, P.; Wessling, M. High Capacity Polyethylenimine Impregnated Microtubes Made of Carbon Nanotubes for CO2 Capture. *Carbon N Y* 2018, *126*, 338–345. https://doi.org/https://doi.org/10.1016/j.carbon.2017.10.023.
(126) Jin, S.; Guo, Y.; Wang, J.; Wang, L.; Hu, Q.; Zhou, A. Carbon Dioxide Adsorption of Two-Dimensional Mo2C MXene. *Diam Relat Mater* 2022, *128*, 109277. https://doi.org/https://doi.org/10.1016/j.diamond.2022.109277.
(127) Wang, B.; Zhou, A.; Liu, F. Carbon Dioxide Adsorption of Two-Dimensional Carbide MXenes. *Journal of Advanced Ceramics* 2018, *7* (3), 237–245.
(128) Mendel, N.; Sîretanu, D.; Sîretanu, I.; Brilman, D. W. F.; Mugele, F. Interlayer Cation-Controlled Adsorption of Carbon Dioxide in Anhydrous Montmorillonite Clay. *Journal*

of Physical Chemistry C 2021, *125* (49), 27159–27169. https://doi.org/10.1021/acs.jpcc.1c06746.
(129) Mendel, N.; Sîretanu, I.; Mugele, F.; Brilman, D. W. F. W. Biogas Upgrading Using Cation-Exchanged Bentonite Clay. *Ind Eng Chem Res* 2023, *62* (43), 17883–17892. https://doi.org/10.1021/acs.iecr.3c01635.
(130) Mendel, N.; Sîreţanu, D.; Sîreţanu, I.; Brilman, D. W. F. W.; Mugele, F. CO2 Adsorption on Variably Hydrated Cation-Exchanged Montmorillonite-Rich Clays. *Journal of Physical Chemistry C* 2025, *129* (14), 6953–6966. https://doi.org/10.1021/acs.jpcc.4c07731.
(131) Cavalcanti, L. P.; Kalantzopoulos, G. N.; Eckert, J.; Knudsen, K. D.; Fossum, J. O. A Nano-Silicate Material with Exceptional Capacity for CO2 Capture and Storage at Room Temperature. *Sci Rep* 2018, *8* (April), 11827. https://doi.org/10.1038/s41598-018-30283-2.
(132) Bø Hunvik, K. W.; Loch, P.; Wallacher, D.; Kirch, A.; Cavalcanti, L. P.; Rieß, M.; Daab, M.; Josvanger, V.; Grätz, S.; Yokaichiya, F.; Knudsen, K. D.; Rodrigues Miranda, C.; Breu, J.; Fossum, J. O. CO2 Adsorption Enhanced by Tuning the Layer Charge in a Clay Mineral. *Langmuir* 2021, *37* (49), 14491–14499. https://doi.org/10.1021/acs.langmuir.1c02467.